Medicinal Chemistry and Molecular Modeling: An Integration To Teach Drug Structure–Activity Relationship and the Molecular Basis of Drug Action

ARTICLE *in* JOURNAL OF CHEMICAL EDUCATION · MARCH 2005

Impact Factor: 1.11 · DOI: 10.1021/ed082p588

3 AUTHORS, INCLUDING:

Carvalho Ivone
University of São Paulo
69 PUBLICATIONS **1,173** CITATIONS
SEE PROFILE

Lílian Bernardes
Federal University of Santa Catarina
16 PUBLICATIONS **137** CITATIONS
SEE PROFILE

Molecular Modeling Exercises and Experiments

edited by
Ronald Starkey
University of Wisconsin–Green Bay
Green Bay, WI 54311-7001

Medicinal Chemistry and Molecular Modeling: An Integration To Teach Drug Structure–Activity Relationship and the Molecular Basis of Drug Action

Ivone Carvalho,* Áurea D. L. Borges, and Lílian S. C. Bernardes
Faculdade de Ciências Farmacêuticas de Ribeirão Preto, Universidade de São Paulo, Av. do Café s/n, Monte Alegre, Ribeirão Preto - SP, 14040-903, Brazil; **carronal@usp.br*

Modern molecular-modeling techniques are remarkable tools in the search for potentially novel therapeutic agents, by helping to understand and predict the behavior of molecular systems. The powerful modeling components, including molecular graphics, computational chemistry, molecular database, and statistical modeling (quantitative structure activity relationship; QSAR) have assumed an important role in the development and optimization of leading compounds. Moreover, current information on the three dimensional (3D) structure of proteins and their functions provide a possibility to understand the relevant molecular interactions between a ligand and a target macromolecule. As a consequence, a comprehensive study of drug structure–activity relationships can help identify a 3D pharmacophore model as an aid for rational drug design. Although this is now a routine approach in medicinal chemistry there are still difficulties in teaching fundamental concepts to undergraduate pharmacy students, such as those related to the molecular-recognition process *(1, 2)*.

An active-learning strategy in medicinal chemistry involves the incorporation of molecular-modeling techniques to assist undergraduate students in the understanding of structure–activity principles. This article focuses on the use of computational chemistry and the protein data bank (PDB) *(3)*, to understand and predict the chemical and molecular basis involved in the drug-receptor interactions. A comprehensive study of structure–activity relationships comprises three approaches. The first approach involves comparative analysis of antimetabolite drugs and the corresponding metabolites (named substrates), by representing, visualizing, and superimposing their 3D structures, obtained by minimization processes and molecular-alignment techniques. Secondly, numerical properties of these molecules are then calculated, the most common being molecular energies and physical constants as partition coefficients, dipolar moments, molecular volumes, and interatomic distances. Thirdly, particular structural features between substrate and antimetabolite are explored by assessing the electrostatic and geometric patterns required for chemical interaction in the active site of the target molecule, obtained from PDB. Table 1 lists some therapeutic areas of interest, such as antineoplastic, anti-HIV, antibiotic, antihypertensive, anti-inflammatory, cholinergic and antihyperlipidemic drugs, associated important enzymes and their corresponding substrates, some relevant PDB files, and antimetabolites currently used as therapeutic agents *(4)*.

3D Structure Comparisons and Overlays

Using the Molecular Modeling Pro *(5)* program it is possible to construct for comparative purposes, favored, low-energy conformations of the substrate and inhibitor. These are optimized by reducing the energy of the molecules in some systematic way until a minimum-energy conformer is found. Minimization processes can correct unfavorable bond lengths,

Table 1. Classes of Drugs, Some Key Enzyme Targets with Their Substrates and Some Associated Antimetabolites, and PDB Files Related to the Enzyme Structures

Group	Therapeutic Class	Enzyme	Substrate	Drug[a] or Antimetabolite	PDB File
I	Antineoplastic	Thymidylate synthase	Deoxyuridylate monophosphate	2′-deoxy-5-fluorouridylate monophosphate (FdUMP)	1tsn
II	Anti-HIV	Reverse transcriptase	Deoxythymidylate monophosphate	Nevirapine	1fkp
III	Anti-HIV	HIV Protease	Polyprotein	Saquinovir	1fb7
IV	Antibiotic	Transpeptidase and Carboxypeptidase	Acil-D-ala-D-ala	Cefotaxime	1cef
V	Antihyperlipemic	HMGO–CoA reductase	HMGO-CoA	Simvastatin	1hw9
VI	Antihypertensive	Dopa descarboxylase	L-Dihydroxyphenylalanine	Dopamine	5pah
VII	Antineoplastic	Dihydrofolate reductase	Dihydrofolic acid	Methotrexate	1rg7
VIII	Anti-inflammatory	Cyclooxygenase	Arachidonic acid	Indomethacin	4cox
IX	Cholinergic	Acetylcholinesterase	Acetylcholine	Tacrine	1dx4

[a]The files describe the following enzymes complexed with an inhibitor or a substrate: 1tls, 1hzn, 1hzw, 1kzi, 1hvy, 1bq1, 1cif, 1tsw (thymidilate synthase); 1cot, 1cou, 1dtq, 1hmv, 1hvu (reverse transcriptase); 1hvp,1kzk, 2aid,2bpv, 2bpw, 7upj (HIV protease); 1ceg, 1es2, 1es3 (transpeptidase and carboxypeptidase); 1dqa, 1hw8, 1hwj, 1qax, 1qay (HMGO-CoA reductase); 1js3, 1js6, 4pah, 1phh, 1d7l (dopa descarboxylase); 1rb3, 1rh3, 1ra3, 7dfr, 3dfr (dihydrofolate reductase); 1dcx, 1cqe, 1cvu, 1ddx, 1cx2, 1pgf (cyclooxygenase); 2ace, 1gqr, 2ack, 2clj, 1qti (acetylcholinesterase).

bond angles, torsion angles and nonbounded interactions in a starting structure, creating a more stable conformation. Mathematical models that perform geometry optimization are divided into classical, mechanical, and quantum mechanical approaches. In computational chemical simulations, the simplified description is a calculated potential-energy surface, which applies classical-mechanics equations to molecular nuclei, without considering electrons. A set of equations and parameters is called force field and most molecular-modeling programs can choose among several force fields, such as MM2 and AMBER *(6)*. The energy of any atomic arrangement can be calculated stepwise, by assessing how the energy of the system varies as the positions of the atoms change. The Molecular Modeling Pro can also generate and examine automatically many molecular conformations, and their corresponding interconversion energy barriers can be plotted. At the completion of the conformational analysis the molecule is placed in its low-energy conformation. Both the stepwise and automatic procedures can be interactively performed to optimize the geometry of the molecules. Structures can then be compared by overlaying appropriate atoms or functional groups, previously aligned in the atomic coordinates. Rotation and different representation forms (by charge or lipophilicity) of the model allow a detailed investigation of the conformational and electronic properties of two structures, which could be the substrate and antimetabolite (inhibitor).

In this article two classes of antineoplastic drugs are chosen to exemplify the structure visualization and superposition processes, which involve compounds that act on the target enzymes thymidylate synthase (TS, Figure 1) and dihydrofolate reductase (DHFR, Figure 2). The purpose of

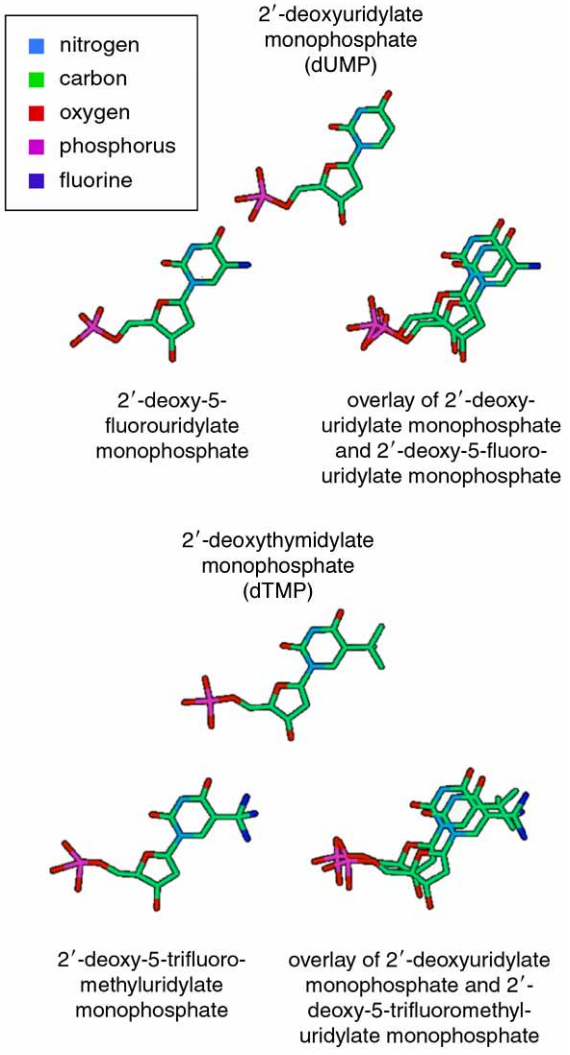

Figure 1. Superposition and comparisons of nucleotide derived antineoplastic drugs, such as 2′-deoxy-5-fluorouridylate monophosphate and 2′-deoxy-5-trifluoromethyluridylate monophosphate, capable of inhibiting TS, with the substrates dUMP and dTMP, respectively.

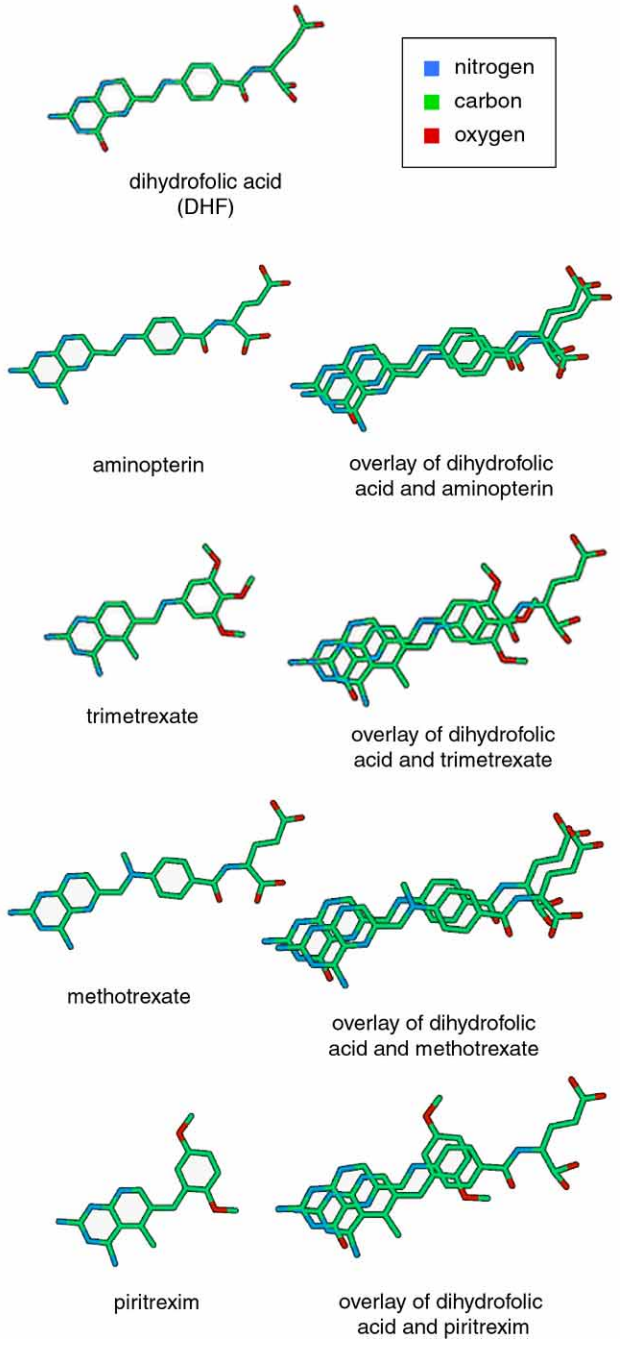

Figure 2. Superposition and comparisons of folate cofactor derived antineoplastic drugs capable of inhibiting DHFR, with the substrate DHF.

Table 2. Physicochemical Similarities and Differences of TS Antimetabolites and Substrate

Compound	Molecular Volume/ (cm^3 mol^{-1})	Log P (Fragment Method)[a]	Dipole Moment/D
2′-Deoxyuridylate monophosphate	140.68	-4.13	4.60
2′-Deoxy-5-fluorouridylate monophosphate	140.33	-5.23	4.43
2′-Deoxythymidylate monophosphate	147.58	-3.48	3.05
2′-Deoxy-5-trifluoromethyluridylate monophosphate (trifluoridine MP)	161.64	-3.24	4.95

[a]Log P is the log of the *n*-octanol/water partition coefficient.

this exercise is to provide a geometrical and chemical overview of the great structural similarity in the substrate and inhibitor. At the same time it emphasizes the importance of considering chemical transformations of a key substrate in a biochemical pathway when developing antimetabolite drugs.

Molecular Dimensions and Properties

Varying the physical and chemical properties of metabolite has often been used in drug design to produce a structure analog, such as an antimetabolite (metabolite antagonism), required for inhibition of cellular growth and response processes. Bioisosterism strategies are frequently used to convert a key substrate into an inhibitor, allowing extra binding interaction to a target enzyme. Substituent modifications can affect various parameters in a drug molecule such as the partition coefficient, electronic density, conformation, bioavailability, and its capacity to establish direct interaction in the receptor domain. Thus, both drug and substrate physical properties can be calculated and compared to give useful information on structure–activity relationships. Important properties can be estimated in the molecular-modeling program, exemplified by partial charges, bond order, dipole moment, ionization potential, electron-density distribution, solubility, and thermodynamic properties. Some of the physical properties including volume, surface area, density, molecular length, and dipole moment are affected by geometry, which depends on the minimization process. Additionally, appropriate orientation of the molecule in the *xy* plane is required for molecular-length comparisons.

Some physical similarities and differences among antineoplastic compounds (Table 1) belonging to groups I (TS) and VII (DHFR) are illustrated, respectively, in Tables 2 and 3. Compared with substrates uridylate and thymidylate, both antimetabolites 5-fluorouracil and trifluridine contain additional electronegative groups, which contribute to better nucleophilicity towards the thymidylate synthase target (Table 2). Fluorine is often considered an isostere of hydrogen. The atom is virtually the same size as hydrogen but more electronegative and thus can be used to vary the drug electronic properties without having any steric effect. Estimates of log P (log of the *n*-octanol/water partition coefficient) by using the fragment method show the greater lipophilic character of fluorinated antimetabolites, as compared with the corresponding substrates (Table 2). Substituting fluorine for enzymically labile hydrogen can also disrupt the catalytic reaction since C−F bonds are not easily broken *(7)*.

In contrast to the dihydrofolate substrate, the antagonist methotrexate has an extra pteridine ring amino group, which improves the hydrogen bond interaction on the active site. Replacement of the 4-oxo group of the substrate by the amino group will not appreciably change the size of the analog, but will have a marked effect on its polarity, electronic distribution, and bonding (Table 3). However, the N-methyl group present in methotrexate induces a different molecular shape compared to dihydrofolic acid and can increase log P and liposolubility. The steric hindrance generated by the methyl group may create constraints and impose particularly favorable conformations for ligand–receptor interactions. Moreover, the presence of the N-methyl group leading to a tertiary amine structure disfavors solvation of a protonated form and favors nonionized forms, which are less soluble in water *(8)*.

The development of resistance during acute leukemia therapy is probably due to the loss of the methotrexate cellular transport mechanism. Thus, investigation for a more lipophilic inhibitor led to trimetrexate and piritrexim, which are independent of the cell-transport mechanism. They are analogs of methotrexate, in which one or two pteridine ring nitrogen atoms are replaced by carbon and a more lipophilic group replaces the benzoylglutamic acid chain. Table 3 lists log P values, showing the greater trimetrexate and piritrexim liposolubility and lower polar surface area, as compared to classical antimetabolites.

Identifying Enzyme 3D Pharmacophores

Many drugs are effective by interacting with biological macromolecules such as enzymes, DNA, glycoproteins, or receptors. The target enzyme–substrate, –inhibitor or –cofactor (ligand) 3D complexes, can be downloaded from PDB onto a computer program and studied by molecular modeling. Ligand and target interactions may be due entirely to noncovalent forces such as electrostatic, hydrogen bonding, and hydrophobic interaction, but occasionally a covalent interaction may be involved. Tight-binding ligands often have a high degree of target complementarity, which can be as-

Table 3. Physicochemical Similarities and Differences of DHFR Antimetabolites and Substrate

Species	Molecular Volume/ (cm^3 mol^{-1})	Log P (Fragment Method)	Dipole Moment/D	Polar Surface Area/$Å^2$
Dihydrofolic acid	224.90	-3.60	5.24	224.86
Aminopterin	223.21	-4.00	4.06	228.81
Methotrexate	234.42	-3.32	3.61	220.02
Trimetrexate	192.97	-0.02	1.53	104.41
Piritrexim	177.25	0.90	4.72	109.17

sessed and measured. A 3D pharmacophore specifies the group spatial relationships, corresponding to a set of features common to active molecules, such as hydrogen-bond donors and acceptors, positively or negatively charged groups, and hydrophobic groups of an appropriate size. The correlation of these structures with pharmacological action and analysis of the complementary molecular interaction between biological molecules and substrate or drug are made possible by the use of a computer-based tool, Protein Explorer, which is accessed from the PDB Internet site, under the option "View Structure". Students wishing to utilize the approach described in this article to study drug–protein interaction via molecular modeling will need to access the Supplemental Material[W] that describes the steps involved in the manipulation of the Protein Explorer program.

Within our own teaching program we ask students to access enzymes from the PDB in different formats and 3D representations and search the "Display File" list to access the catalytic site. Although some target enzyme active sites are not available from PDB files, students estimate how strongly a molecule will bind to a catalytic site by selecting the ligand's surface contacts favorably interacting with specific functional groups of both ligand and macromolecule (see Supplemental Material[W]). TS (group I) and DHFR (group VII) are convenient enzymes to illustrate these tutorials owing to their cooperative action in the cell de novo biosynthesis of thymidilate nucleotides.

Both enzymes have long been recognized as a drug target for inhibiting DNA synthesis in rapidly proliferating cells such as cancer cells or in bacterial or malarial infections. Traditional inhibitors, clinically used as antineoplastic and antimicrobial agents, have been modeled on 2′-deoxyuridine monophosphate or the cofactor N^5,N^{10}-methylenetetrahydrofolate, and thus are structurally related to natural substrate and cofactor *(4)*.

Thymidylate Synthase

Background

Thymidylate synthase catalyzes the reductive methylation of 2′-deoxyuridine monophosphate (dUMP) to 2′-deoxythymidylate monophosphate (dTMP), using N^5,N^{10}-methylenetetrahydrofolate cofactor, which is concomitantly converted to 7,8-dihydrofolate (DHF). Dihydrofolate reductase and serine hydroxymethyltransferase are required by the cell to transform consumed coenzyme back to the active N^5,N^{10}-methylenetetrahydrofolate form. The pathway is illustrated in Figure 3.

Based on background information, the student draws the initial steps of the catalytic mechanism as shown in Scheme I *(9)*. By this mechanism the reaction proceeds by the catalytic Michael addition of a cysteine residue (Cys 146) to C-6 of dUMP, generating the dUMP enolate, able to attack either the cyclic or open form of methylenetetrahydrofolate. Apparently, the preferred way is the much more reactive Mannich basic form of the 5*N*-iminium ion of methylenetetrahydrofolate, allowing the formation of a dUMP- and cofactor-containing ternary complex, covalently binding the enzyme. Deprotonation of the C-5 proton of dUMP, assisted by a basic tyrosine residue (Tyr 94), is the next step giving rise to tetrahydrofolate (THF) and a dUMP derivative containing an exocyclic methylene group C-5, still bound to the

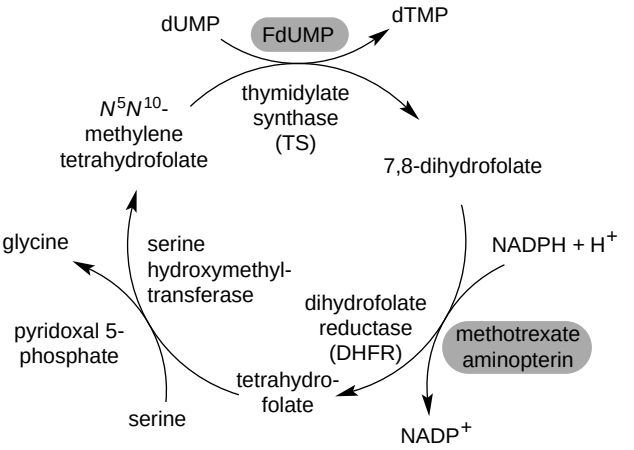

Figure 3. Cell thymidylate biosynthetic pathway involving the enzymes TS, DHFR, and serine hydroxymethyltransferase. Potential inhibitors of key steps are also indicated with shading.

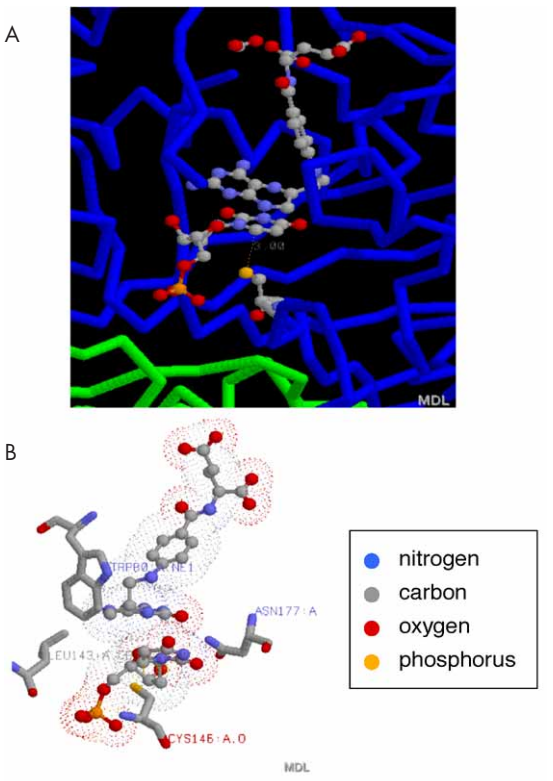

Figure 4. (A) Images obtained from PDB file 1kzi, showing tight contact between the cofactor, tetrahydrofolate (top), and the substrate, 2-deoxyuridylate monophosphate (middle). Cysteine residue (Cys 146) is represented at the bottom, positioned for attack on substrate C-6. (B) Cofactor and substrate are drawn in balls and sticks and the amino acid residues in sticks.

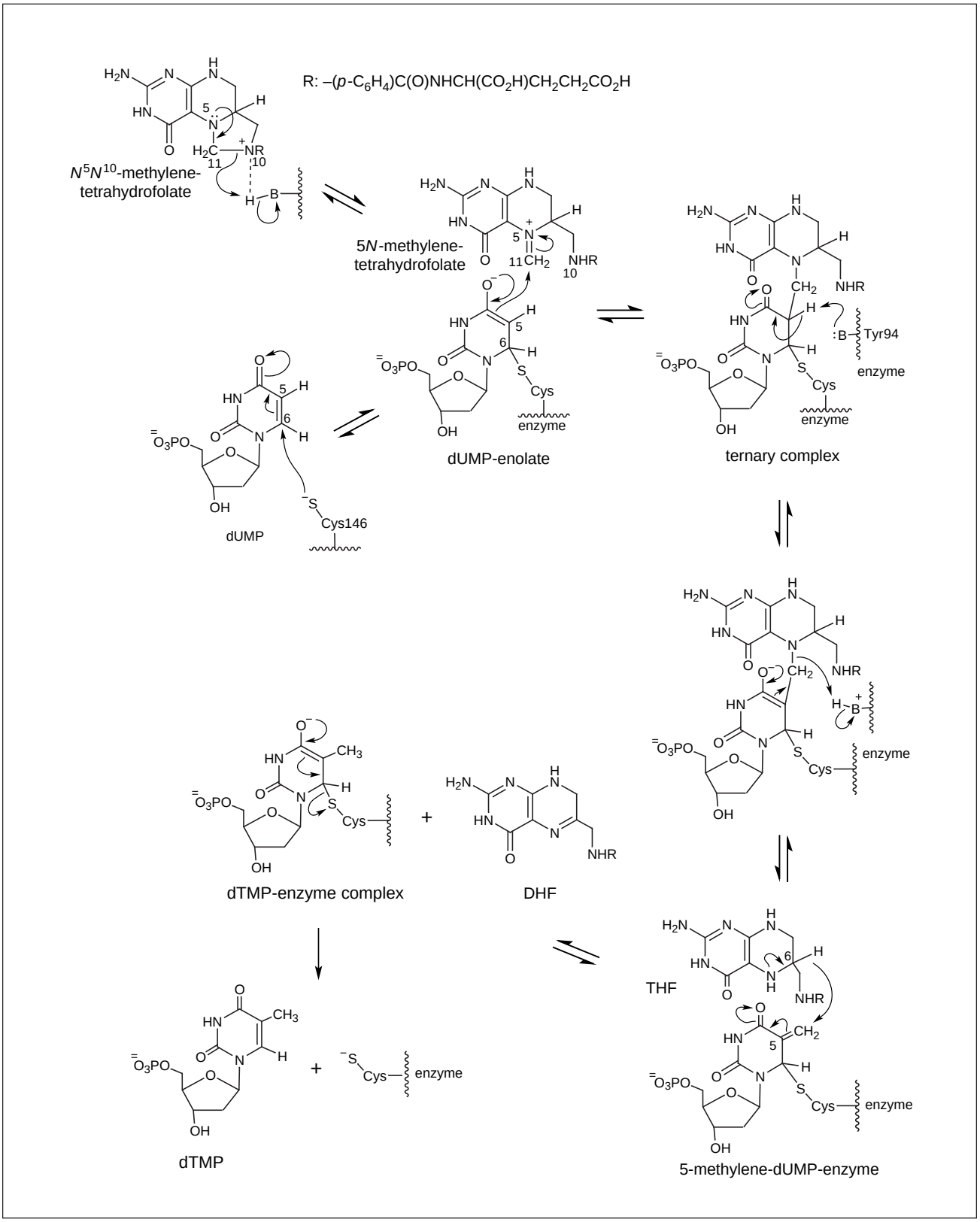

Scheme I. Proposed mechanism for the thymidylate synthase-catalyzed reaction.

enzyme. Finally, the C-5 exocyclic methylene group may be reduced by the transfer of a hydride from C-6 in THF to give a dTMP-enzyme enolate and dihydrofolate (DHF), probably facilitated by the proper alignment of the orbital of the C-6 hydrogen bond with the exo-methylene group (Scheme I).

Tutorial

A Protein Explorer contact analysis of the enzyme–substrate complex, PDB entry 1kzi from *E. coli*, revealed both the ligand binding place and the binding interactions between substrate and cofactor *(10)*. Indeed, long-range recognition factors between drug and receptor represented by hydrogen bonds may be assessed and inferred in terms of electrostatic character and steric orientation. Figure 4A shows the bent conformation tetrahydrofolic acid with its *p*-aminobenzoic acid (PABA) residue above the pteridine ring, allowing tight enzyme and nucleotide binding. In this thymidylate synthase catalyzed reaction, it is possible to visualize the good proximity of cysteine residue (Cys 146) sulphydryl group to the C-6 of dUMP pyrimidine moiety (1.94 Å), and the close contact of the coenzyme, that favors the attachment of the dUMP enolate at C-5. Hydrogen bonds between Cys 146, Arg 166 and Tyr 94, Figure 4B, are also included in the TS structural domain and probably involved in the bond instability of the enzyme covalent adduct for further cleavage. The students are reminded to look at the potential base Tyr 94 and surrounding water that seem involved in the abstraction of the pyrimidine ring C-5 proton of the ternary complex, preceding DHF elimination. In addition, the optimal positioning of C-6 THF cofactor and the C-5 dUMP exocyclic methylene group for hydride transfer (2.5Å) and the active site shielding from bulk solvent are influenced by Trp 80 and Leu 143 residues. Although there are other interactions at the catalytic site, the hydrogen bonds between dUMP and the highly conserved amino acid Asn 177, which encode dUMP specificity over other nucleotides, should be pointed out.

The elucidation of the mechanism of thymidylate synthase was through the structure determination of the complex formed when 5-fluoro-2′-deoxyuridylate monophosphate (5FdUMP) inactivates the enzyme; the reaction involved is shown in Scheme II and can be viewed by the structures from PDB entry 1tls, also from *E. coli (11)* (Figure 5).

The presence of fluorine in place of labile hydrogen may disrupt the enzymatic reaction since C−F bonds are not easily broken. Its target enzyme accepts antineoplastic 5-fluorouracil, metabolically converted to 5-fluoro-dUMP (FdUMP), since it appears little different from the normal uracil substrate. However, the mechanism of the enzyme-catalyzed reaction is totally disrupted since fluorine can not leave the molecule as does the original hydrogen attached to C-5 of dUMP, which leaves as a positively charged species. As a result, a stable covalent complex is formed, linking inhibitor, cofactor, and enzyme, as a result of the strong fluorine electron-withdrawing potential (Scheme II). The covalently linked complex undergoes an extensive conformational change, resulting in a structure containing the C-11 to C-5 methylene bridge between the tetrahydrofolate residue and FdUMP, which lies axial to the pyrimidine ring, in a similar configuration of thiol linkage between Cys 146 and C-6 of FdUMP *(11)*.

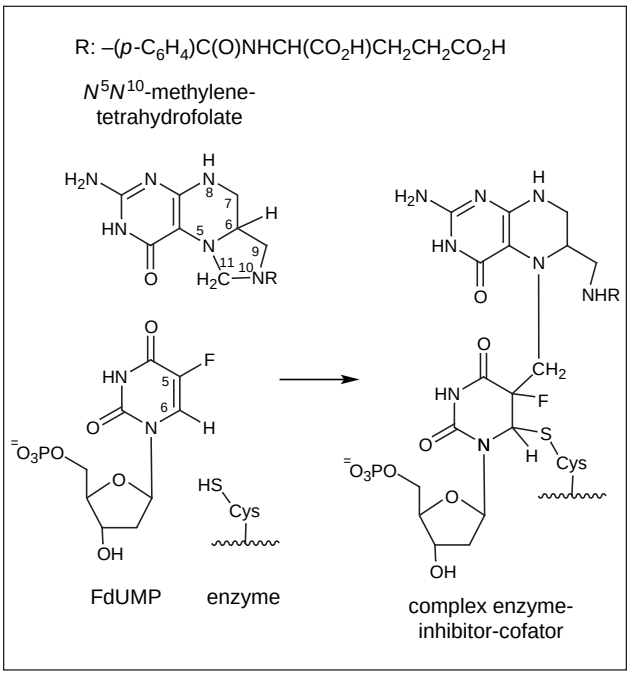

Scheme II. Inactivation of thymidylate synthase by FdUMP (2′-deoxy-5-fluorouridylate monophosphate).

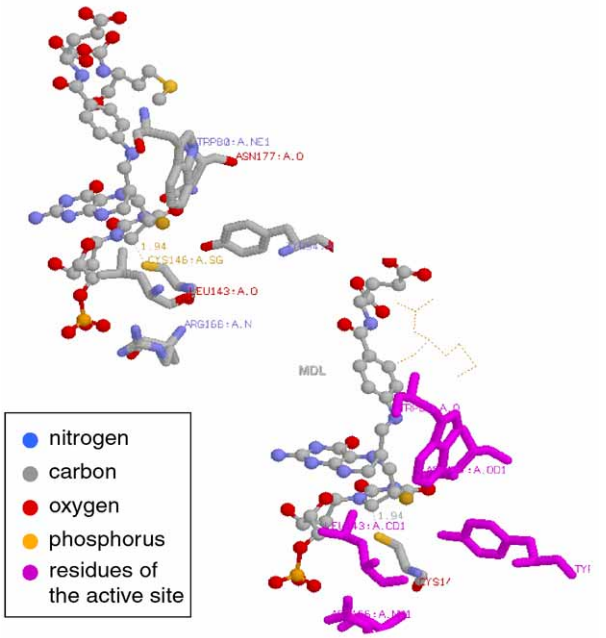

Figure 5. Images obtained from PDB file 1tls, showing the dihydrofolate cofactor (top), and the inhibitor, 2′-deoxy-5-fluorouridylate monophosphate (middle), bound by covalent linkage in the active site of thymidylate synthase. The cysteine residue (Cys146) is represented at the bottom, positioned to attack C-6 FdUMP. Cofactor and inhibitor are drawn in balls and sticks, and the amino acid residues in sticks. The left side picture shows the target amino acids in a uniform gray scale.

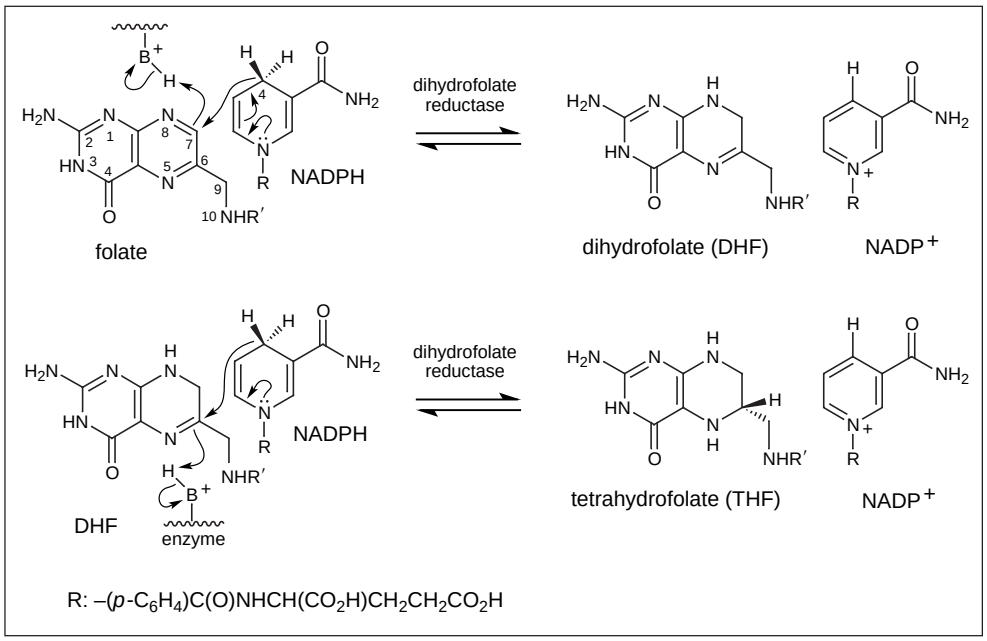

Scheme III. Dihydrofolate reductase-catalyzed reductions of folate and dihydrofolate in the presence NADPH cofactor.

Dihydrofolate Reductase

Background

The effect of dihydrofolate antagonists on DNA synthesis results partially from dihydrofolate reductase (DHFR) inhibition, which depletes the N^5,N^{10}-methylenetetrahydrofolate pool, limiting thymidylate (dTMP) biosynthesis. Furthermore, the inhibition of enzyme additionally hinders nucleic acid biosynthesis by lowering the level of 10*N*-formyltetrahydrofolate, the formyl donor to glycinamide ribonucleotide in purine biosynthesis.

Two of the folic acid C−N double bonds are reduced stepwise by the nicotinamide adenine dinucleotide phosphate (NADPH)-dependent enzyme dihydrofolate reductase to produce tetrahydrofolate, which is recycled by reoxidation. The students draw the 2D stepwise reduction of folic acid to dihydrofolic and tetrahydrofolic acids in the presence of NADPH-dependent enzyme dihydrofolate reductase *(9),* as illustrated in Scheme III.

Thus, the students learn that tetrahydrofolate is not the full coenzyme; the complete coenzyme form contains an additional carbon atom between the N-5 and N-10 positions,

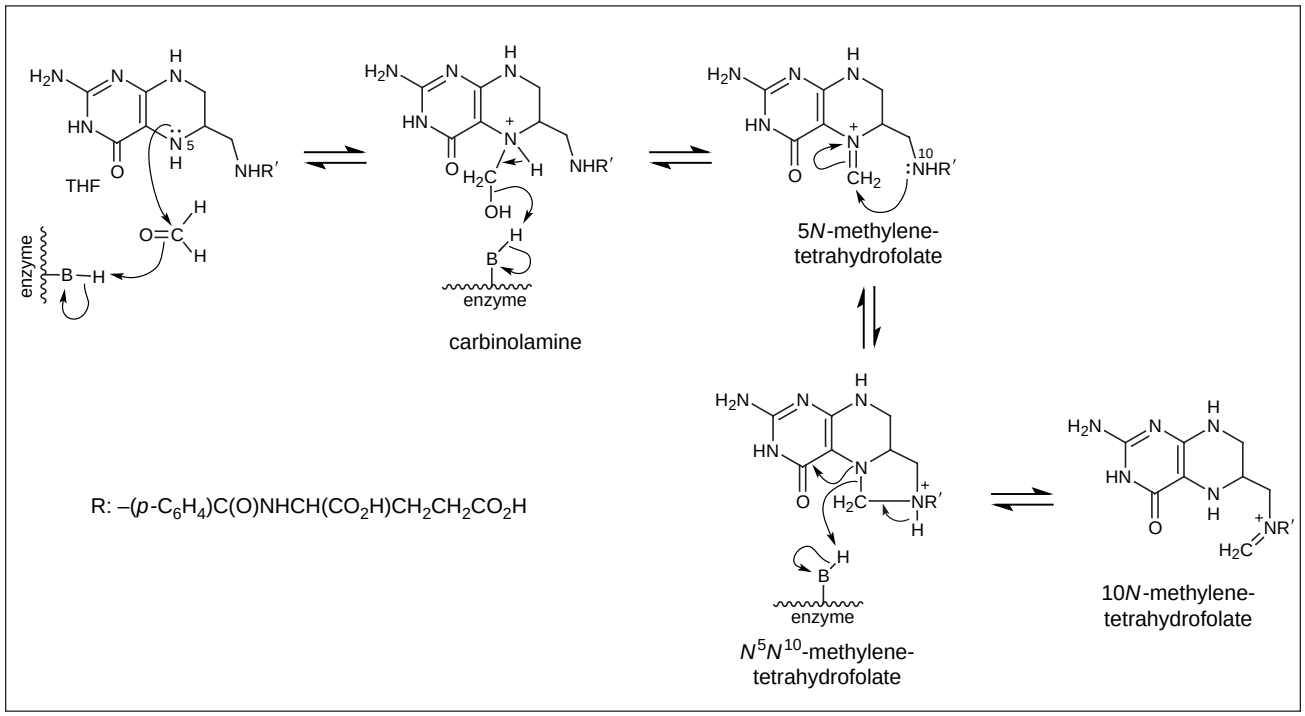

Scheme IV. Serine hydroxymethyltransferase-catalyzed reaction of formaldehyde and tetrahydrofolate giving methylenetetrahydrofolate.

provided by a formaldehyde molecule derived from the L-serine methylene group. Serine hydroxymethyltransferase catalyzes the attack of the more basic tetrahydrofolate N-5 nitrogen on the formaldehyde group, giving 5*N*-methylenetetrahydrofolate, by dehydration of the carbinolamine intermediate. N^5,N^{10}-methylenetetrahydrofolate and 10*N*- and 5*N*-methylenetetrahydrofolate cofactors are in equilibrium but the former is more abundant owing to the closer proximity between the 10*N*-amino group and 5*N*-methylene group (Scheme IV).

Tutorial

Dihydrofolate reductase is included in at least ninety 3D structures in the PDB, in many of which it is complexed to folic acid (substrate), $NADP^+$ (cofactor), or inhibitors. Different organisms show slight differences in the structural features of the enzyme, but the DNA building function remains intact. To understand folate binding to the active site and the important differences between substrate and inhibitor binding interactions, the students search PDB enzyme structures bound to folate and $NADP^+$ and, for comparison, the same structure bound to methotrexate, as an inhibitor (antimetabolite) that replaces and mimics folate. The major amino acid residues of the protein, which make nonbonded contacts with $NADP^+$-folate and $NADP^+$-methotrexate, may be visualized and inferred in terms of electrostatic and steric properties.

The folate-$NADP^+$-enzyme complex, obtained from PDB entry 7dfr as a crystal structure of *E. coli*, has a long groove showing folate bound at one end, and $NADP^+$ at the other end *(12)*. By using the Protein Explorer tools, it is possible to visualize most of the energetically favorable binding interactions in the ternary $NADP^+$-folate complex. Figure 6 illustrates the main interactions between folate and $NADP^+$, such as the van der Waals contacts between the pteridine ring and the nicotinamide moiety. DHFR sidechains are wrapped around these two molecules, positioning them tightly next to one another (3.3 Å) and making it easier for the hydride to be transferred from C-4 in the nicotinamide NADPH moiety to C-6 of the folate dihydropteridine ring. The tight contact can not be relieved owing to the close proximity of Phe 31 to the pteridine ring in one side, forming a strong hydrophobic interaction above the binding site (3.2 Å), and of Tyr 100 close to the NADP-nicotinamide on the other side *(12)*.

As can be seen from Figure 6, dihydrofolate, in a bent conformation in a deep hydrophobic cleft, binds to a single polar residue, Asp 27, leading to two distorted H-bonds, with N-3 (2.6 Å) and the 2-amino group (3.2 Å) of folate. These interactions confer rigidity to the bound substrate and promote hydrophobic interactions with residues, such as Phe 31, Ile 5, and Met 20. Asp 27 is also important for substrate N-5 protonation, via a water molecule, which increases the carbonium ion character at C-6 NADPH, facilitating the hydride transfer. Figure 6 also shows the substrate positioned at the catalytic site by H-binding the 2-amino and 4-oxo groups to two ordered water molecules, Wat 301 and Wat 206, which are, respectively, hydrogen bonded to the conserved residues Thr 113 and Trp 22, and acting as a hydrogen bonding bridge to Asp 27. The greater specificity of the enzyme for dihydrofolate reduction as compared to folate can be explained by the extra H-bonding interaction of the N-8 donor proton of dihydrofolate, not present in the folate, with the closer carbonyl group of Ile 5 (Figure 7A). The *p*-aminobenzoyl moiety of the substrate occupies a hydrophobic pocket formed by residues Phe 31, Leu 28, and Leu 54. Finally, a pair of hydrogen bonds completes the binding of the glutamyl group involving its carboxyl and the Arg 57 guanidinium groups.

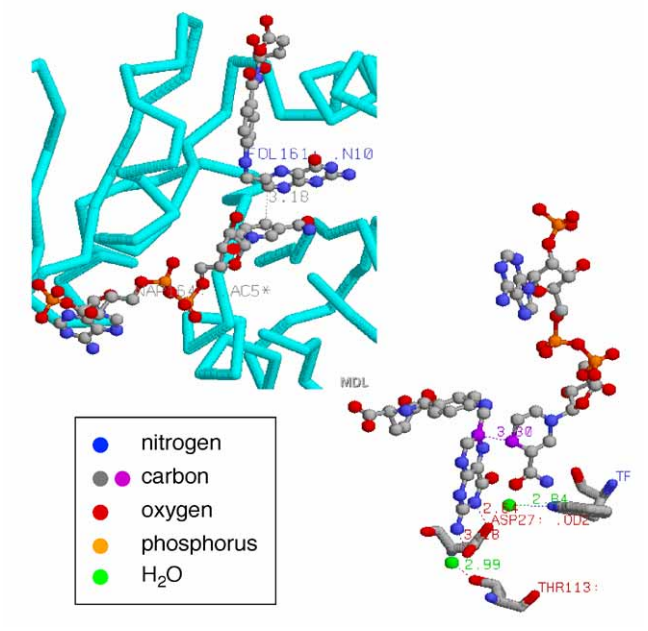

Figure 6. Images from PDB file 7dfr, showing tight contacts between substrate (folate) and cofactor ($NADP^+$) on the dihydrofolate reductase active site. Cofactor and substrate are drawn in balls and sticks, amino acid residues in sticks and water as a single ball.

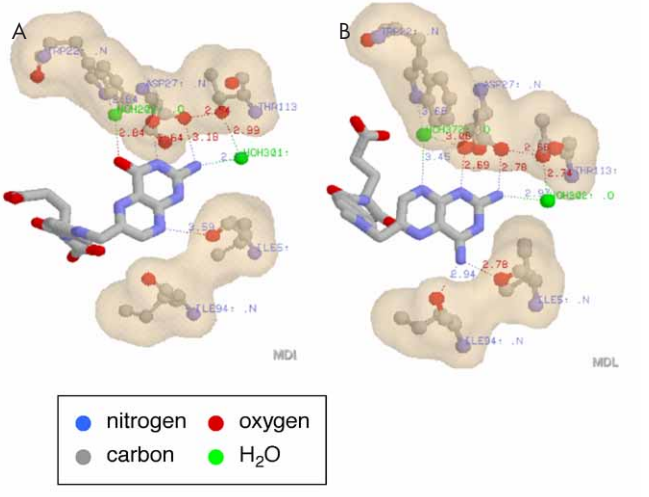

Figure 7. Main interactions of (A) substrate (dihydrofolate) and (B) inhibitor (methotrexate) on the dihydrofolate reductase active site. Images from PDB entries 7dfr and 1ra3, using Protein Explorer tools. Substrate and inhibitor are drawn in stick, amino acids in ball and stick, colored by contact surface, and water as a single ball.

On the other hand, the oxidized coenzyme $NADP^+$ in an extended conformation appears to have more favorable interactions with DFHR through the pyrophosphate and the ADP 2′-phosphate groups. These are illustrated by ten hydrogen bonds, one ionic interaction (His 45) and two helix dipoles in the case of pyrophosphate, and five hydrogen bonds and one ion pair (Arg 44) with ADP 2′-phosphate *(12).* It should be clear that the nicotinamide mononucleotide is held in the enzyme by hydrogen bonds (Arg 7 and Ile 14), dipole and van der Waals interactions (Ile 94, Tyr 100, and Thr 46), and the 14–19 backbone of the Met 20 loop closing over the bound nicotinamide ribose. The Met 20 loop changes from the closed to the occluded conformation during the catalytic cycle, in movements that allow tetrahydrofolate release, assisted by NADPH binding *(13).*

Both, the 4-amino-4-deoxy antimetabolites of folic acid, aminopterin, and its 10*N*-methyl homologue, methotrexate, bind tightly to the enzyme site through the 2,4-diaminopteridine ring, protonated at the physiological pH. These inhibitors are folate mimics because of their similar size, shape, chemical composition, and binding position. Although the inhibitor complex has almost identical overall geometry, it binds to dihydrofolate reductase a thousand times more tightly than folate, blocking the action of the enzyme. The substrate binding interactions around the pteridine portion are inverted due a rotation of approximately 180° about an axis through the N-5 and 2-amino group and distorted when compared to the bound methotrexate. This can be seen by assessing PDB files entries 7dfr (dihydrofolate) *(12)* and 1ra3 (methotrexate) *(14),* both obtained from *E. coli* (Figure 7). The 2-amino groups of both ligands form two hydrogen bonds with Asp 27 and Wat 301 (dihydrofolate) or Wat 302 (methotrexate). The distortion of pteridine substrate allows its N-3 group to be H-bonded to Asp 27 (Figure 7A), while methotrexate prefers to position N-1, allowing the H-binding of N-8 to Wat 372, instead of binding to Ile 5. As a result, the extra 4-amino group on methotrexate takes the place of N-8 of the substrate and favors better contacts with the enzyme, involving two concomitant H-bindings to Ile 5 and Ile 94 (Figure 7B).

A great deal of information is provided by these overall visualizations, concerning ligand–enzyme interactions and comparisons between substrate and inhibitor specificity. It is assumed that the *p*-aminobenzoyl-L-glutamate group of both substrate and methotrexate is bound in the same manner at the DHFR catalytic site.

Concluding Remarks

Molecular modeling has been an essential tool in the teaching of relevant aspects of medicinal chemistry such as structure–activity relationships and the molecular bases of antimetabolites or drug action. The 3D visualization and identification of enzymic 3D pharmacophores, provided by advanced graphic systems (Protein Explorer) and PDB improve the students understanding of the biological event by correctly predicting the binding affinity of a ligand to its target macromolecule. Also, by exploring the steric and electrostatic patterns involved in drug action, the students enhance their perception and appreciation of molecular-recognition processes and their applications to drug design. Furthermore, computational chemistry offered visual insights and the great deal of information obtained from PDB help the students to improve their scientific communication skills, such as 3D illustrations and animations in the final seminar presentations.

Supplemental Material

Tutorials of Molecular Modeling Pro and Protein Explorer to perform the described exercises are available in this issue of *JCE Online*.

Acknowledgments

The authors thank Zuleika Rotschield for valuable comments on the manuscript and the investigators who elucidated the 3D structures of target enzymes and deposited in the Protein Data Bank.

Literature Cited

1. Cohen, C. N. *Guidebook on Molecular Modeling in Drug Design;* Academic Press: San Diego, CA, 1996.
2. Leach, A. R. *Molecular Modeling: Principles and Applications;* Longman: Essex, United Kingdom, 1996; pp 543–585.
3. RCSB Protein Data Bank. *http://www.rcsb.org/pdb* (accessed Dec 2004).
4. Gringauz, A. *Introduction to Medicinal Chemistry: How Drugs Act and Why;* Wiley-VCH: New York, 1997.
5. Quinn, J. A. *Molecular Modeling Pro 4.05: Computational Chemistry Program;* ChemSW Inc: Fairfield, CA, 2001.
6. Sansom, C. E.; Smith, C. A. *Biochem. Educ.* **1998,** *26,* 103–110.
7. Wermuth, C. G. *The Practice of Medicinal Chemistry;* Wermuth, C. G., Ed.; Academic Press: San Diego, CA, 1996, pp 226–228.
8. Bajorath, J.; Kraut, J.; Li, Z.; Kitson, D. H.; Haglet, A. T. *Proc. Natl. Adac. Sci*. **1991,** *88,* 6423–6426.
9. Silverman, R. B. *The Organic Chemistry of Enzyme-Catalyzed Reactions;* Academic Press: San Diego, CA, 2000; pp 479–500.
10. Fritz, T. A.; Liu, L.; Finer-Moore, J. S.; Stroud, R. M. *Biochemistry* **2002,** *41,* 7021–7029.
11. Hyatt, D. C.; Maley, F.; Montfort, W. R. *Biochemistry* **1997,** *36,* 4585–4594.
12. Bystroff, C.; Oatley, S. J.; Kraut, J. *Biochemistry* **1990,** *29,* 3263–3277.
13. Sawaya, M. R.; Kraut, J. *Biochemistry* **1997,** *36,* 586–603.
14. Bolin, J. T.; Filman, D. J.; Mattews, D. A.; Hamlin, R. C.; Kraut, J. *J. Biol. Chem.* **1982,** *257,* 13650–13662.